Journal of Hydrology 553 (2017) 763–772

Contents lists available at ScienceDirect

Journal of Hydrology

journal homepage: www.elsevier.com/locate/jhydrol

Research papers

Retention performance of green roofs in representative climates worldwide

F. Viola *, M. Hellies, R. Deidda

DICAAR, Università di Cagliari, Via Marengo 2, Cagliari, Italy

ARTICLE INFO

Article history:
Received 3 March 2017
Received in revised form 28 July 2017
Accepted 21 August 2017
Available online 31 August 2017
This manuscript was handled by Marco borga, Editor-in-Chief, with the assistance of Yasuto Tachikawa, Associate Editor

Keywords:
Greenroof
Retention

ABSTRACT

The ongoing process of global urbanization contributes to an increase in stormwater runoff from impervious surfaces, threatening also water quality. Green roofs have been proved to be innovative stormwater management measures to partially restore natural states, enhancing interception, infiltration and evapotranspiration fluxes. The amount of water that is retained within green roofs depends not only on their depth, but also on the climate, which drives the stochastic soil moisture dynamic. In this context, a simple tool for assessing performance of green roofs worldwide in terms of retained water is still missing and highly desirable for practical assessments.

The aim of this work is to explore retention performance of green roofs as a function of their depth and in different climate regimes. Two soil depths are investigated, one representing the intensive configuration and another representing the extensive one. The role of the climate in driving water retention has been represented by rainfall and potential evapotranspiration dynamics. A simple conceptual weather generator has been implemented and used for stochastic simulation of daily rainfall and potential evapotranspiration. Stochastic forcing is used as an input of a simple conceptual hydrological model for estimating long-term water partitioning between rainfall, runoff and actual evapotranspiration. Coupling the stochastic weather generator with the conceptual hydrological model, we assessed the amount of rainfall diverted into evapotranspiration for different combinations of annual rainfall and potential evapotranspiration in five representative climatic regimes. Results quantified the capabilities of green roofs in retaining rainfall and consequently in reducing discharges into sewer systems at an annual time scale. The role of substrate depth has been recognized to be crucial in determining green roofs retention performance, which in general increase from extensive to intensive settings. Looking at the role of climatic conditions, namely annual rainfall, potential evapotranspiration and their seasonality cycles, we found that they drive green roofs retention performance, which are the maxima when rainfall and temperature are in phase.

Finally, we provide design charts for a first approximation of possible hydrological benefits deriving from the implementation of intensive or extensive green roofs in different world areas. As an example, 25 big cities have been indicated as benchmark case studies.

1. Introduction

The continuous growth of impervious surface areas leads to increased downstream flows with critical consequences for the functioning of existing sewer systems and triggers water quality degradation in receiving water bodies (Carter and Jackson, 2007; Carter and Rasmussen, 2006). A variety of management practices have been proposed to limit the environmental pressures associated with the altered hydrology of urban areas. In this context, green roofs are an innovative solution for mitigation of the impact of stormwater runoff, with the advantage of recovering green spaces, while preserving environmental quality (Getter and Rowe, 2006). Green roofs are indeed a valid alternative to traditional stormwater design and a low impact development practice (Dietz, 2007). Several authors recommend the use of vegetative roofs as an attractive stormwater management practice in urban watersheds, in order to reproduce the benefits produced by the interception and evapotranspiration processes in the natural water cycle, as in less disturbed environments. Green roofs are now quite familiar in Europe and North America: some cities have built green roof pilot projects and adopted incentives for applying green roof

* Corresponding author.
E-mail address: viola@unica.it (F. Viola).

http://dx.doi.org/10.1016/j.jhydrol.2017.08.033
0022-1694/

practices (Dvorak and Volder, 2010), while standards and guidelines are also being set up.

Several environmental benefits can be associated with green roofs, mainly related to the reduction of building energy consumption, mitigation of urban heat island effect, improvement of air quality, water management, increase of sound insulation, and ecological preservation (Berardi and Ghaffarian Hoseini, 2014). An important benefit related to green roofs is that they can efficiently detain and retain stormwater when compared to conventional roofs. In the following we analyze some scientific studies aimed at the evaluation of hydrological performance of green roofs by distinguishing between field experiments and modelling approaches.

Many field experiments have been carried out in order to understand the hydrological behaviour of green roofs and to quantify the water-related benefits in specific climatic and physical conditions. An interesting case has been proposed by Carter and Rasmussen (2006): a paired green roof-black roof test plot was constructed at the University of Georgia (USA) and monitored for one year for the effectiveness of the green roof in reducing stormwater flows. Green roof precipitation retention decreased with precipitation depth; ranging from about 90 percent for small storms to slightly less than 50 percent for larger storms. Moreover, they also found that runoff from the green roof was delayed and that the average runoff lag times increased.

Bengtsson et al. (2005) studied a thin extensive green roof and its water balance in southern Sweden. They observed that runoff from the green roof is substantially reduced when compared to the runoff from black roofs because of evapotranspiration. As a physical interpretation of the water dynamics within the green roof, they associated the beginning of runoff with the condition of soil moisture reaching or exceeding the field capacity, and estimated the consequent runoff as equal to the precipitation excess. They argued that the daily runoff dynamics could be described as a function of daily precipitation, potential evapotranspiration and storage capacity of the green roof.

Czemiel Berndtsson (2010) made a critical review of green roof performances on the basis of results from full-scale installations as well as from laboratory models and looked for factors affecting runoff dynamics. She concluded that geometrical properties (mainly slope), climate (mainly rainfall) and vegetation (its age) are fundamental in determining runoff from green roofs.

Feng et al. (2010) quantified the energy balance components within an extensive green roof installation in the South China University of Technology in Guangzhou (China). They found that, without water limitations, incoming solar radiation was diverted into evapotranspiration of the plant-soil system (60%), long-wave radiation exchange between the canopy and the atmosphere (30%) and net photosynthesis of plants (10%).

Performance of green roofs have been also investigated in the Mediterranean climate by Fioretti et al. (2010) with two full-scale experiments in north-west and central Italy. They concluded that green roofs significantly mitigate storm water runoff generation in terms of runoff volume reduction, peak attenuation and increase of concentration time, although reduced performance could be observed during high precipitation periods. Under subtropical climate conditions, Voyde et al. (2010) analyzed field monitoring results from a large extensive green roof in Auckland, New Zealand (NZ). They found that the green roof retained about 82% of rainfall received per rainfall event, with a median peak flow reduction of 93% compared to rainfall intensity. Similarly to other studies, also Voyde et al. (2010) identified in rain depth, rain intensity, climatic variables and antecedent dry days the main key factors influencing the hydrology of green roofs.

DeNardo et al. (2005) studied a green flat roof at Rock Springs, Pennsylvania (USA). They observed a range of rainfall retention from 19% to 98% in seven storms and peak runoff delayed by 2 h. The effect of slope on extensive green roof stormwater retention was instead analyzed by Getter et al. (2007) using 12 extensive green roof platforms constructed at the Michigan State University (USA). They demonstrated that the lower the slope the higher the retention, with an average retention value of about 80%.

Monterusso et al. (2004) analyzed runoff from four commercial green roof systems containing three distinct vegetation types at the Michigan State University (USA). Rainfall retained during their experiments ranged from 39% to 58%. It is worth noticing that their results highlight how differences in water retention can be attributed to substrate depth, rather than drainage system or vegetation type.

Two studies made in the UK by Stovin (2010) and Stovin et al. (2012) demonstrated the important role of mean rainfall intensity, rainfall depth and an antecedent dry weather period, which conditions antecedent moisture conditions. The latter is indeed crucial in determining the performance of green roofs, in terms of retentions, peak attenuation and delay under extreme rainfall conditions.

If field experiments, as briefly referred to above, allow the underlying physical processes to be understood, modelling approaches permit phenomena to be mimicked, and consequently to simulate green roof performances even in unmonitored conditions. Hydrological modelling demonstrated that widespread green roof implementation can significantly reduce peak runoff rates, particularly for small storm events (Carter and Jackson, 2007).

Hilten et al. (2008) modelled stormwater runoff data from green roofs with the HYDRUS- 1D model (Šimůnek et al., 2008) in order to determine peak flow, retention and detention time for runoff. Storm data were collected on a green roof in Athens, Georgia, USA, and used to calibrate HYDRUS-1D simulated runoff. The study site consisted of a 37 m^2 modular block green roof containing engineered soil and vegetation including several sedum species. Simulations highlight the role of rainfall depth in determining water retention: in fact small storms are fully retained while larger storms are partially attenuated.

The work carried out by Palla et al. (2009) advanced the understanding of the unsaturated water flow in the coarse-grained porous media usually employed in green roofs. Using a bidimensional model based on Richards' law and the Van Genuchten-Mualem functions they were able to simulate the variably saturated flow within the green roof system with a satisfactory reproduction of hydrograph main features, i.e. total discharged volume, peak flow, hydrograph centroid and water content. In a later study, the same authors compared the performance of HYDRUS-1D with those obtained by a conceptual linear reservoir in reproducing the hydrologic response of a green roof system within the urban environment (Palla et al., 2012). They found that, comparing simulations with observations from a field site in Genova, Italy, the HYDRUS-1D model resulted more reliable. However, prediction errors of the conceptual model were still limited, so that outflow hydrographs in terms of both total effluent volume and hydrograph shape were predicted with acceptable accuracy.

While most of the previous mentioned studies focused on event scale or short time windows, there are few examples in literature of long-term green roof performance evaluations, mainly approached with hydrological models. An interesting study in this context was proposed by Stovin et al. (2013). They used a conceptual hydrological flux model for the long term continuous simulation of retention performance of extensive green roofs at 4 locations in the UK, with different annual rainfall (ranging from 500 to 2700 mm/year) and potential evapotranspiration (from 618 to 700 mm/year). A long term analysis was also performed by Carson et al. (2013) who simulated extensive green roof performance in NY using an empirical model, calibrated against observations and forced by historical rainfall (1971–2010). Locatelli et al.

(2014) used a deterministic lumped rainfall–runoff conceptual model to simulate the hydrological response of green roofs during a 22-year (1989–2010) continuous simulation with Danish climate data. Cipolla et al. (2016) used field data to calibrate and validate a numerical model, namely the commercial software SWMM 5.1, to simulate the long-term hydrologic response of an extensive green roof.

Although the growing interest in the adoption of green roofs has attracted the attention of many researchers who focused on the crucial hydrological phenomena emerging from field observations and the hydrological modelling problem, as briefly reviewed above, many studies were restricted to specific areas of interest. In this framework, results presented in this manuscript aim to quantify retention performance of green roofs worldwide, considering several climatic conditions. In order to do that a simplified stochastic weather generator has been proposed and described in Section 2.1. This model has been designed to mimic daily rainfall and potential evapotranspiration in different climates. In particular, it is able to reproduce stationary or seasonal forcings, which in turn have been used to feed a simple conceptual green roof model, which is described in Section 2.2. The role of soil substrate in governing water retention at an annual time scale has been investigated considering an intensive and an extensive configuration. Results have been summarized in Section 3, where design charts for different climatic conditions are also provided for a rapid first approximation estimate of green roof retention performance worldwide.

2. Methods

2.1. Weather generator

The use of a weather generator has always been related to the need of producing indefinitely long synthetic weather series by simulating key properties of observed meteorological records (Wilby, 1999). The pioneering idea of using Poisson point process and clustered point processes to simulate the occurrences of rainfall events at different time scales dates back to the eighties (Rodriguez-Iturbe et al., 1987a; Rodríguez-Iturbe et al., 1987b). During the last thirty years, in order to capture and reproduce rainfall properties better across wide ranges of temporal and spatial scales, there has been considerable research in the field of rainfall modelling using stochastic point processes, which can be mainly classified as Neyman-Scott and Barlet-Lewis model types (Burlando and Rosso, 1991; Cowpertwait et al., 2002; Cowpertwait et al., 1996; Cowpertwait, 1991; Cowpertwait and O'Connell, 1997; Entekhabi et al., 1989; Islam et al., 1990; Puente et al., 1993; Verhoest et al., 1997). Sometimes however, for sake of simplicity or analytical tractability, the temporal structure within each rain event has been ignored and the marked Poisson process representing precipitation has been physically interpreted at a daily time scale, where the pulses of rainfall correspond to daily precipitation assumed to be concentrated at an instant in time (Laio et al., 2001). We followed this last approach and integrated it with a simple parametric representation proposed by Milly (1994) to describe the essential features of the annual land surface hydrologic forcings. The model assumes that the seasonality of climate is mainly driven by the seasonality of the solar irradiance normal to the top of the atmosphere, which produces a strong signal with a dominant period of one year in most climatic variables. Precipitation and potential evapotranspiration time series have been thus simulated as stochastic processes with expected values modelled with annual harmonics, according to main climatic features observed in 10,000 observational sites worldwide.

The occurrence of rainfall R at time t is idealized as a series of events at a daily time scale, arising from a non-stationary and cyclic Poisson point process with parameter $1/\lambda$ (rate of the Poisson process occurrences, [1/days]) and whose interarrival time λ (t) [days] is here modelled through a cyclic sinusoidal function, with 1-year period, according to the following equation:

$$\lambda(t) = \bar{\lambda}\left[1 + \delta_\lambda sin\left(\frac{2\pi t}{365} + \omega_\lambda\right)\right] \quad (1)$$

where $\bar{\lambda}$ is the average interarrival time [days] between rainfall events, the standardized semi-amplitude δ_λ is the ratio between the semi-amplitude of the annual harmonics of λ(t) and the annual average (i.e. $\bar{\lambda}$.), while ω_λ. is the initial phase.

Rainfall rates during each event are assumed to be a random process described by an exponential distribution, with mean α (t) [mm/day] described as follows:

$$\alpha(t) = \bar{\alpha}\left[1 + \delta_\alpha sin\left(\frac{2\pi t}{365} + \omega_\alpha\right)\right] \quad (2)$$

where $\bar{\alpha}$ is the average amount of rainfall [mm/day], the standardized semi-amplitude δ_α is the ratio of the semi-amplitudes of the aual harmonics of $\alpha(t)$. to the annual average (i.e. $\bar{\alpha}$), and ω_α. is the inial phase.

Potential evapotranspiration $ET_p(t)$ [mm/day] has been modelled with a harmonic as follows:

$$ET_p(t) = \overline{ET}_p\left[1 + \delta_E sin\left(\frac{2\pi t}{365} + \omega_E\right)\right] \quad (3)$$

where $\overline{ET}_p$ is the average annual potential evapotranspiration [mm/day], the standardized semi-amplitude δ_E. is the ratio of the semi-amplitude of the annual harmonics of $ET_p(t)$. to the annual average (i.e. $\overline{ET}_p$), and ω_E. is the initial phase.

We decided to reduce the degrees of freedom of this analysis to simulate green roof performance at an annual time scale as a function of only two climatic variables (i.e. $\overline{P}$ and $\overline{ET}_p$) while keeping the problem as simple as possible. In order to do that, it is worth noting that the same expected annual precipitation $\overline{P}$ [mm/year] can be obtained by the infinite combination of $\bar{\alpha}$ and $\bar{\lambda}$., as shown e.g. in Fig. 1. Thus we decided to keep constant the mean interarrival time $\bar{\lambda}$. for all the simulated climatic conditions while exploring

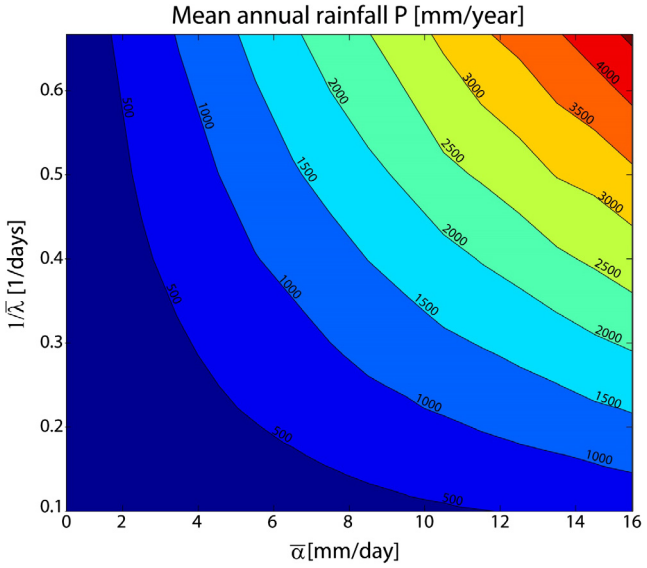

Fig. 1. Expected annual rainfall depths as a function of average interarrival time $\bar{\lambda}$ and average amount of rainfall $\bar{\alpha}$ as obtained by integration of Eqs. (1) and (2) with parameters δ_λ = 0.45; δ_α = 0.35; $\omega_\lambda = -\pi/2$; $\omega_\alpha = \pi/2$.

the variability of $\overline{\alpha}$; consequently, different values of $\overline{P}$ will be obtained using the stochastic model of Eqs. (1) and (2).

In order to apply our model with a reliable parametrization in different climatic conditions, we explored the parameter space by fitting Eqs. (1)(3) to observed time series downloaded by the GHCN (Global Historical Climatology Network, https://www.ncdc.noaa.gov/oa/climate/ghcn-daily/) database, which pooled daily climate data from land surface stations across the globe. We focused the attention on daily precipitation and temperature da, using the 10,000 stations with longest time series. The location of the selected stations is reported in Fig. 2.

With reference to rainfall, daily data from each station have been first analyzed at a monthly time scale in order to determine the average rainfall amount α on wet days, the mean number of occurrences and consequently the rate of the Poisson process $1/\lambda$. (estimated as the number of rainy days divided by the days in the month). The average values $\overline{\alpha}$ and $\overline{\lambda}$ have been thus estimated as the arithmetic mean from the monthly time series. For each year, the semi-amplitudes of the annual harmonic of α and

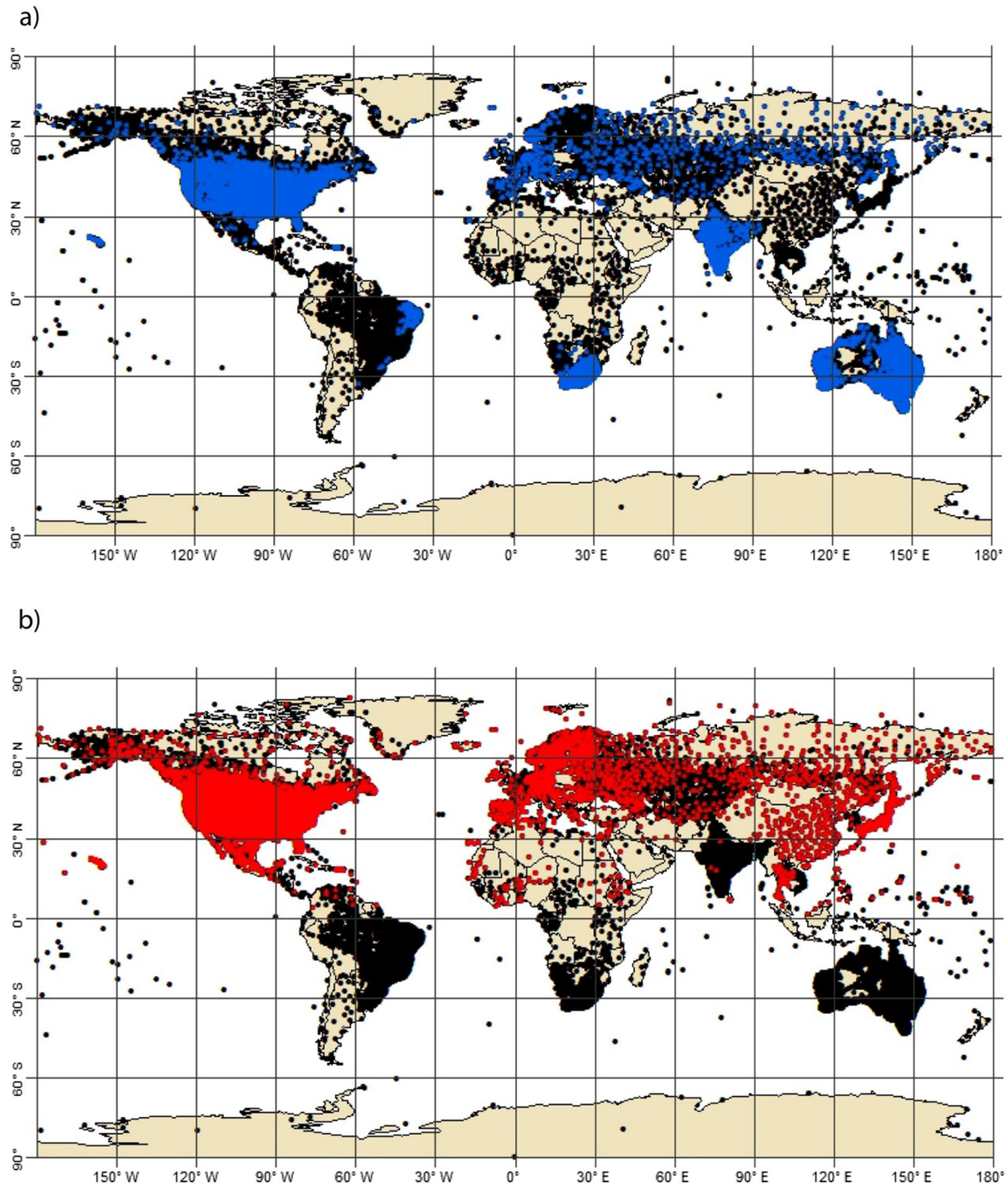

Fig. 2. Location of the 10,000 rainfall (a) and temperature (b) gauging stations used to parameterize the weather generator (Data from https://www.ncdc.noaa.gov/oa/climate/ghcn-daily).

λ have been computed as the half of the difference between maximum and minimum values assumed at a monthly time scale. Parameters δ_λ and δ_α. have been finally estimated as the ratio between the mean of semi-amplitudes over all years and annual averages $\overline{\alpha}$ and $\overline{\lambda}$. Estimated parameters $\overline{\lambda}$, $\delta\lambda$, $\overline{\alpha}$, δ_λ, for all the 10,000 considered stations, have been reported as histograms in Fig. 3a–d.

Daily temperature data have been used to obtain potential evapotranspiration also taking into account solar insulation at the selected stations. Specifically, for each station, temperature observations have been averaged at a monthly time scale and then a monthly ET_p. time series has been assessed by a simplified procedure as a function of temperature and station latitude (Thornthwaite, 1948). Similarly to Eqs. (1) and (2), for parameterization of Eq. (3) average value $\overline{ET_p}$ has been estimated as the mean of monthly ET_p. time series in each station, while the standardized semi-amplitude δ_E has been estimated as the ratio between the mean of semi-amplitudes over all years and annual average $\overline{ET_p}$.

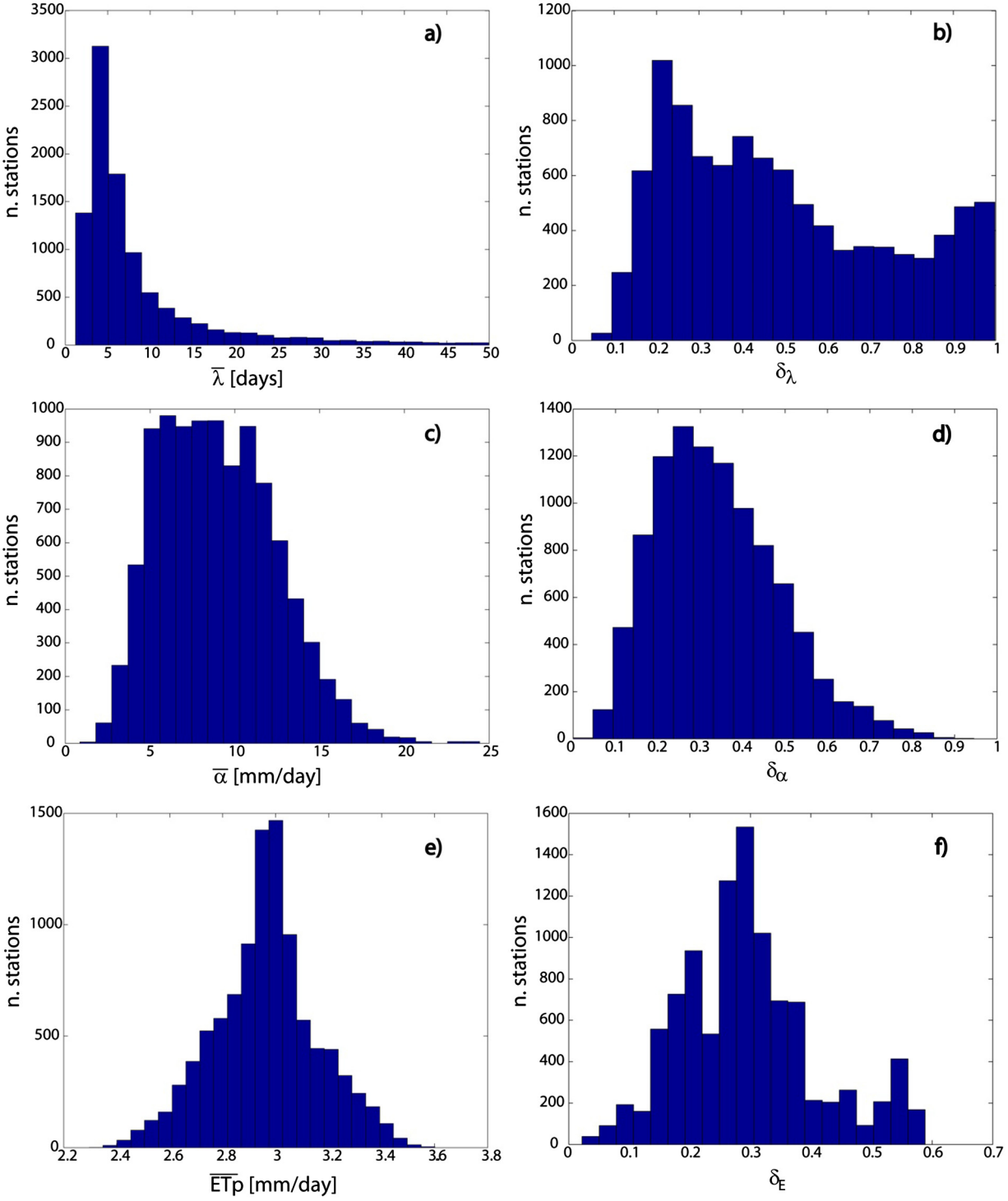

Fig. 3. Worldwide statistics from the 10,000 selected sons for: average rainfall interarrival time $\overline{\lambda}$ (a) and corresponding standardized semi-amplitude δ_λ. (b); average amount of rainfall $\overline{\alpha}$ (c) and corresponding standardized semi-amplitude δ_α. (d); average potential evapotranspiration $\overline{ET_p}$ (e) and corresponding standardized semi-amplitude δ_E (f).

Fig. 3e shows annual averages $\overline{ET_p}$ obtained in the selected locations and reveals a quite symmetric distribution, while the standardized semi-amplitude δ_E. of the annual harmonic is shown in Fig. 3f.

We decided to keep $\overline{\lambda}$ constant for all simulations in order to keep the degree of freedom of the problem low. On the basis of our investigations, we assumed $\overline{\lambda}$ equal to 4.35 days, that is the median value observed in the 10,000 considered stations (Fig. 3a). We then considered five representative climatic regimes, hereafter named also cases. The first is characterized by constant rainfall rates and potential evapotranspiration during t hydrological year, in the second and third cases only one of the two varies, while in the latter two both climatic forcings are cyclic (in phase or in counter-phase). With the same intention to keep our set up simple, cyclic time series have been built keeping constant also the standardized semi-amplitudes of $\overline{\lambda}$, α and ET_p, that have been chosen as the median of their empirical distributions, i.e. $\delta_\lambda = 0.45$, $\delta_\alpha = 0.35$, $\delta_E = 0.30$. Estimated parameters have been summarized in Table 1, where they are combined in order to depict five different climatic regimes.

T weather generator has been used to generate a 100-year-long rainfall and potential evapotranspiration daily time series for all the possible combinations of $\overline{\alpha}$ and $\overline{ET_p}$ for each climatic regime. Time series have been used as input to the conceptual hydrological model, discussed below.

2.2. Runoff model

The hydrological conceptual model introduced by Viola et al. (2014) has been used to simulate soil moisture dynamics in the soil layer and consequently an evapotranspirative flux and runoff from green roofs. Although the model has been developed for natural river basins, slight changes allow the conceptual scheme to be adapted to our setting, following a similar approach as in former studies that applied conceptual models for simulating the hydrological behaviour of green roofs (Palla et al., 2012).

Three interconnected elements have been used: a soil bucket linked with two linear reservoirs, one accounting for the surface runoff component over the roofs, and another accounting for the leakage collection and release. The runoff contribution per unit area has been calculated at a daily time scale, considering the sewer connection as the basin outlet. The runoff over the green roofs, although they are usually designed to limit and possibly avoid it, has been modelled by saturation excess and then transferred to the sewer system through the surface reservoir with a transit time of a day. Water leaked from the top soil layer is ideally collected by a second reservoir characterized again by a residence time of one day. It is worth mentioning that although both the transit and residence times are certainly less than one day, they are both set to one day according to the time step of the adopted models.

The water input to the system is the daily rainfall depth, R [mm/day], which drives the relative soil moisture dynamics. Soil is characterized by porosity and by root depth, termed n and Z_r respectively, whose product, known also as "active soil depth", will be used as a model parameter. The numerical solution of a simple balance equation, through a forward finite differences method, allows the calculation of soil moisture variation within the soil bucket during a daily temporal step. The runoff over the green roof (Q_s) occurs when rainfall exceeds the available storage capacity and is equal to the excess. The water losses due to evapotranspiration ET and leakage $L = (s - s_t)nZ_r$ are calculated at each time step as a function of the relative soil moisture (s) as follows:

$$ET + L = \begin{cases} 0 & if\ s \leqslant s_0 \\ ET_p\left(\frac{s-s_0}{s_t-s_0}\right) & if\ s_0 < s \leqslant s_t \\ ET_P + (s - s_t)nZ_r & if\ s_t < s \leqslant 1 \end{cases} \quad (4)$$

where s_t has a role of field capacity and s_0 represents the wilting point. The evapotranspiration-leakage-soil moisture relation is modelled assuming that when relative soil moisture exceeds s_t, evapotranspiration occurs at the maximum rate, ET_p ., while saturation water $(s - s_t)nZ_r$ is transferred instantaneously to the conceptual linear reservoir. Below s_t, no leakage occurs and evapotranspiration decreases linearly to zero for relative soil moisture equal to s_0 or less. As already pointed out by Viola et al. (2016), the relation in Eq.(4) between the soil moisture and water losses is simple and parsimonious because it uses only three parameters, two characterizing the soil properties (s_t and s_0) and one representing the maximum (or potential) evapotranspiration rate ET_p. In order to take into account the influence of vegetation on water demand, a vegetational coefficient should be introduced. However, the virtual vegetation variability (as defined e.g. by Viola et al. (2014)) would introduce another degree of complexity to the problem; thus we preferred to consider a single vegetation type that will be used for both intensive and extensive green roofs.

T total runoff Q is simply computed as the sum of two contributions: the excess saturation surface runoff, Q_s, and the leakage, L. Each contribution is routed into a linear reservoir characterized by a one-day residence time.

Model outputs have been aggregated at a yearly time scale and then averaged to estimate an index of retention (IOR) defined as the ratio between actual evapotranspiration and rainfall for each 100-year-long time series. This index can range between zero (no evapotranspiration, green roofs are ineffective) and one (all the rain is diverted into evapotranspiration, thus the green roof has a perfect efficiency in reducing water inputs to the sewer system). The IOR has been calculated in the five representative climatic regimes, introduced in Section 2.1, and referring to two green roof configurations. The first is an extensive one, thus a thin layer of active soil (depth of 90 mm), while the second is an intensive configuration characterized by a deeper soil ($nZ_r = 450$ mm). Both the analyzed configurations have the same soil hydrological properties and same vegetation; thus the same parameters $s_0 = 0.30$ and $s_t = 0.70$ have been adopted in Eq. (4) for both configurations.

Table 1
Weather generator parameters used in Eqs. (1)(3) to simulate the five climatic regimes and index of retention (IOR) for the two green roof configurations analyzed.

	$\lambda(t)$			$\alpha(t)$			$ET_p(t)$			Index Of Retention	
	$\overline{\lambda}$ [days]	δ_λ [−]	ω_λ [rad]	$\overline{\alpha}$ [mm/days]	δ_α [−]	ω_α [rad]	$\overline{ET_p}$ [mm/days]	δ_E [−]	ω_E [rad]	nZr 90 mm	nZr 450 mm
Case 1	4.35	0	0	Variable	0	0	variable	0	0	0.529	0.596
Case 2	4.35	0	0	Variable	0	0	variable	0.30	$-\pi/2$	0.518	0.590
Case 3	4.35	0.45	$-\pi/2$	Variable	0.35	$\pi/2$	variable	0	0	0.500	0.572
Case 4	4.35	0.45	$-\pi/2$	Variable	0.35	$\pi/2$	variable	0.30	$\pi/2$	0.519	0.585
Case 5	4.35	0.45	$-\pi/2$	Variable	0.35	$\pi/2$	variable	0.30	$-\pi/2$	0.471	0.545

3. Results

Each of the proposed representative climatic regimes, introduced in Section 2.1, refers to a specific combination of rainfall and potential evapotranspiration during the hydrological year. For each case the influence of annual rainfall $\overline{P}$ (ranging from zero to 3000 mm/year) and potential evapotranspiration $\overline{ET}_p$ (ranging from zero to 2000 mm/year) in leading to annual water retention is explored with reference to extensive (nZ_r = 90 mm) and intensive (nZ_r = 450 mm) green roof configurations. The performances are evaluated in terms of IOR for all the possible $\overline{P} - \overline{ET}_p$ combinations and presented in Fig. 4.

Table 1 reports the averages of the obtained IORs within the chosen domain of rainfall and potential evapotranspiration, to give an indicative performance score that is helpful in comparing the five representative climatic regimes. Furthermore 25 cities have been proposed as benchmark examples. Each of these cities has been attributed to a given climatic case and from graphical analysis of Fig. 4 it is possible to argue about green roof retention performances, for both intensive and extensive configurations, in those selected locations.

The first analyzed case refers to stationary conditions that can be considered as an ideal reference condition: rainfall statistics are supposed to remain unaltered within the hydrological year as well as potential evapotranspiration. Fig. 4, central and right subplots in the first row, presents results in terms of IOR for the two analyzed soil configurations. The average retention observed for all the possible combinations of annual rainfall and potential evapotranspiration is 52.8% for the thin soil and 59.6% for the deep soil, confirming that intensive configurations are more effective in retaining water. This is obviously due to the higher active soil depth, which can store more water, reducing leakages and consequently allowing more water evapotranspiration from soil and vegetation.

The second case is representative of zones where rainfall is almost constant during the hydrological year, but temperature and consequently potential evapotranspiration have one peak as it is, for instance, in oceanic climate. The green roofs performance in these climatic conditions are comparable to those obtained in the steady state case (see Table 1); results in terms of IOR for the two analyzed configurations are shown in Fig. 4, second row. The city of New York falls in this climatic case: in fact the monthly rainfall is almost constant during the year (about 100 mm/month), while temperatures show seasonality, with a peak during the summer (about 23 °C in August) and a trough in winter (about 0° in January). From Fig. 4 it is possible to extract the mean retention efficiency for extensive (i.e. IOR = 0.55) and intensive configuration (i.e. IOR = 0.62) for this city.

In the third case we summarized world areas where potential evapotranspiration could be considered constant through the hydrological year while rainfall shows seasonal patterns with one peak. This is the case for tropical climates. Retention performance in this case decreases: the average percentage of rainfall diverted into evapotranspiration is 49.9% for extensive green roofs and 57.2% for the intensive ones (see Table 1). This drop in performance, with respect to the ideal case 1, is explained by more runoff and leakage produced during the heavy rainfall periods. Results are shown in Fig. 4, third row, and the city of Mumbai could be presented as the paradigm of this climatic situation. Temperature is almost constant during the year (27 °C as daily mean), but rainfall is mostly concentrated during the monsoon period (from June to September). In this city, with this peculiar climate, the mean retention efficiency for intensive green roofs is equal to 0.41 while for extensive configurations is 0.34.

The world areas where both rainfall and temperature display seasonal cycles have been summarized in the last two cases. In case 4 we consider in-phase climatic forcings, meaning that when rain is high, the evapotranspiration demand is high, too. Such a condition occurs in humid subtropical climates. Performances in this case are again comparable with the ideal case 1 (see Table 1). Indeed when rainfall inputs increase also losses due to evapotranspiration increase, keeping soil moisture dynamics similar to those observed in the case 1. Fig. 4, fourth row, depicts the IOR for all the explored combinations of annual rainfall and potential evapotranspiration for the two green roof configurations. Tokyo is one of the cities belonging to this case: the analysis of climatic statistics shows how the temperature has a seasonal behaviour, with a peak in August (average daily mean of about 23 °C) when rainfall has its maximum (about 280 mm/month). Results for this city reveal that extensive green roofs retain 48% of annual rainfall, while intensive ones retain 56%.

The last case refers to areas where rainfall and potential evapotranspiration are in counter-phase during the hydrological year, as happens with a Mediterranean climate. This climatic condition is the worst in terms of retention performances, that are the lowest among the analyzed cases (0.47 for extensive and 0.54 for intensive green roofs). The physical explanation lies in the higher leakage losses occurring in such a climate when potential evapotranspiration is low. Results are shown in Table 1 and Fig. 4, fifth row. Among the analyzed cities, Rome with hot summers (25 °C of daily mean in August) and mild rainy winters (with more than 80% of rain falling from October to April), falls in this latter climatic case.

To give evidence of the reliable results provided by the design charts plotted in Fig. 4, and thus also of the overall good performance of the modelling approach adopted in this study, we refer to the results presented by Stovin et al. (2013) and Carson et al. (2013), already described in the introduction. Namely, we compared the index of retention as obtained by the mentioned authors with those provided by our design charts in Fig. 4. In particular, we first attributed each location studied in Stovin et al. (2013) and Carson et al. (2013) to a climatic case, and then extrapolated the main climatic conditions (i.e. mean annual rainfall and potential annual evapotranspiration) which determined the performance of the analyzed green roofs. Then, we used the design charts in Fig. 4 to calculate the IOR, referring to intensive or extensive configurations depending on the considered case study. Results of these comparisons, which have been reported in Table 2, show a good accordance in very different climatic conditions, with negligible discrepancies between observations and modelled IORs which are mainly attributable to the different soil capacity considered and can certainly be accepted under the assumptions and simplifications here made.

Finally, in order to highlight the role of seasonality in governing the retention performance, a comparison of IOR was plotted in Fig. 5 for the five climatic regimes with the same mean annual rainfall $\overline{P}$ and potential evapotranspiration $\overline{ET}_p$. The Figure highlights how the phase between rainfall and potential evapotranspiration signals controls green roofs performance: in fact when climatic forcings are synchronous, IOR is generally higher. Conversely, when rainfall has intra-annual maxima performance decreases, especially if evapotranspiration is low in that period. Different behaviors emerge when, keeping the same annual rainfall, the potential evapotranspiration increases, amplifying the impact of intra-annual climatic variability on retention performance.

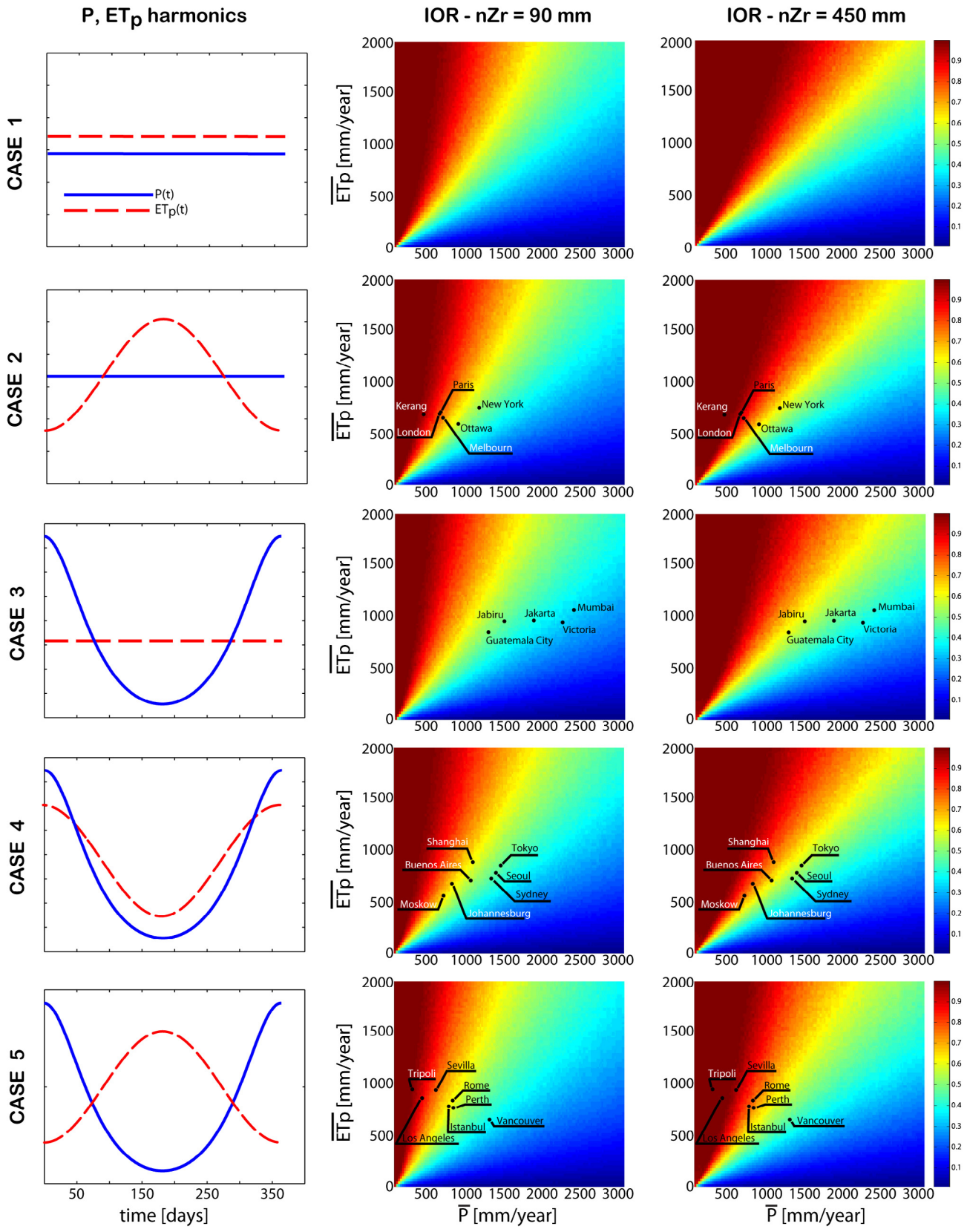

Fig. 4. Green roofs retention performance in different climates (first column) and for two active soil depths: second column refers to extensive configurations (i.e. $nZ_r = 90$ mm) while the third column refers to intensive configurations (i.e.$Z_r = 450$ mm). Results are shown in terms of index of retention IOR ($\overline{ET}/\overline{P}$), as a function of mean aual rainfall $\overline{P}$ and mean annual potential evapotranspiration $\overline{ET}_p$. Dots indicate climatic conditions for selected large cities, to show the simple usage of the design charts for estimation of green roofs performance.

Table 2
Comparison of green roof retention performance as resulted from literature studies and from the design charts given in Fig. 4.

Location	Case (1–5)	$\overline{P}$ [mm/year]	$\overline{ET_p}$ [mm/year]	IOR from Stovin et al. (2013)* and Carson et al. (2013)**	IOR from Fig. 4
NW Scotland	5	2700	620	0.19*	0.2
Sheffield	5	838	670	0.40*	0.5
Cornwall	5	1360	650	0.33*	0.4
East Midlands	2	500	700	0.59*	0.74
New York	2	1290	750	0.58**	0.55

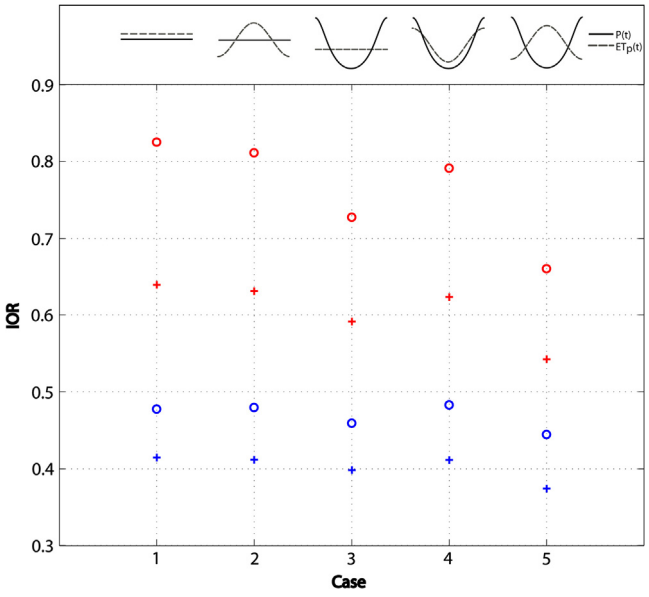

Fig. 5. Index of retention in different climates (five cases, as in Fig. 4), for two active soil depths (circles refer to deep soil, crosses to shallow soil) and for two long-term average conditions of annual rainfall and potential evapotranspiration. Red marks $\overline{P}$ = 1500 mm, $\overline{ET_p}$ = 1500 mm; Blue marks $\overline{P}$ = 1500 mm, $\overline{ET_p}$ = 750 mm. The inset above recalls the intra-annual variability of climatic forcings for the five considered cases.

4. Conclusion

A worldwide assessment of retention efficiency of green roofs has been carried out and presented in this study with the aim to provide information to scientists, practitioners and policy makers involved in urban planning and interested in evaluating the possible hydrological impact of green roofs in areas where this evaluation is tricky or impossible, due e.g. to the lack of climatic data (rainfall and temperature) or the costs of field experiments. Specifically we designed a tool for a first-approximate estimate of green roof retention performance in different climates with respect to intensive and extensive configurations, by coupling a simple stochastic weather generator with a conceptual model miming the hydrological behaviour of the green roof. Massive numerical simulations have been carried out in order to generate rainfall and potential evapotranspiration time series in different climates and afterwards to evaluate hydrological water fluxes through the two green roof configurations.

Results highlight the role of soil depth and climate in driving the retention capacity of a green roof. The amount of retained water increases with increasing soil depth, because more water is allowed to be stored in the active soil and consequently more water can evaporate from soil and vegetation. Regarding the climate, the performance of a green roof increases when rainfall and potential evapotraspiration exhibit the same seasonality during the hydrological year (i.e. their forcings are in-phase), as happens, for example in humid subtropical climates. Conversely, the green roof presents the minimum efficiency when rainfall and potential evapotranspiration are in counter-phase, as is found in a Mediterranean climate.

Moreover, we provided design charts for representative climates worldwide, which make it possible to evaluate quickly green roof performance starting from easy-to-obtain data and climatic information. Monthly rainfall and temperature distribution will guide the user in the choice of the appropriate climatic case as a function of rainfall and temperature stationarity or seasonality within a generic hydrological year. Then the annual mean value of rainfall and potential evapotranspiration are the only required data in order to evaluate how much water is retained by the green roof system, or conversely how much is released into the stormwater sewer system. Two main green roof configurations have been explored, intensive and extensive: for both an evaluation of the index of retention (ranging from 0, when all the rainfall is turned into runoff, to 1, when all the rainfall is retained and evapotranspired) can be read from the corresponding design charts.

Further research efforts are needed in order to examine the role of rainfall extremes in driving green roof retention and detection performance at temporal time scales shorter than a day, which are crucial for sewer system design. This will be challenging for the complexity of extreme rainfall statistics depending not only on site location but also on local conditions as topography or sea distance.

Acknowledgments

This work has been partially funded by *Regione Siciliana – Dipartimento Attività Produttive,* "PO FESR 2007-2013". "*Linea di intervento 4.1.2.a.: Azioni di qualificazione dell'offerta di ricerca e servizi a supporto all'innovazione e al trasferimento tecnologico* (Qualification research actions and services to support innovation and technology transfer)". Project: "*Rete Integrata dei Laboratori Tecnologici delle Università Siciliane – RILTUS*".

References

Bengtsson, L., Grahn, L., Olsson, J., 2005. Hydrological function of a thin extensive green roof in southern Sweden. Nord. Hydrol. 36 (3), 259–268.

Berardi, U., Ghaffarian Hoseini, A., 2014. State-of-the-art analysis of the environmental benefits of green roofs. Appl. Energy 115, 411–428. http://dx.doi.org/10.1016/j.apenergy.2013.10.047.

Burlando, P., Rosso, R., 1991. Comment on "Parameter estimation and sensitivity analysis for the modified Bartlett Lewis rectangular pulses model of rainfall" by S. Islam et al. J. Geophys. Res.: Atmos. 96 (D5), 9391–9395.

Carson, T.B., Marasco, D.E., Culligan, P.J., McGillis, W.R., 2013. Hydrological performance of extensive green roofs in New York City: observations and multi-year modeling of three full-scale systems. Environ. Res. Lett. 8 (2). http://dx.doi.org/10.1088/1748-9326/8/2/024036.

Carter, T., Jackson, C.R., 2007. Vegetated roofs for stormwater management at multiple spatial scales. Landscape Urban Plan. 80 (1–2), 84–94. http://dx.doi.org/10.1016/j.landurbplan.2006.06.005.

Carter, T.L., Rasmussen, T.C., 2006. Hydrologic behavior of vegetated roofs. J. Am. Water Resour. Assoc. 42 (5), 1261–1274.

Cipolla, S.S., Maglionico, M., Stojkov, I., 2016. A long-term hydrological modelling of an extensive green roof by means of SWMM. Ecol. Eng. 95, 876–887. http://dx.doi.org/10.1016/j.ecoleng.2016.07.009.

Cowpertwait, P., Kilsby, C., O'Connell, P., 2002. A space-time Neyman-Scott model of rainfall: Empirical analysis of extremes. Water Resour. Res. 38 (8).
Cowpertwait, P., O'Connell, P., Metcalfe, A., Mawdsley, J., 1996. Stochastic point process modelling of rainfall. I. Single-site fitting and validation. J. Hydrol. 175 (1–4), 17–46.
Cowpertwait, P.S., 1991. Further developments of the Neyman-Scott clustered point process for modeling rainfall. Water Resour. Res. 27 (7), 1431–1438.
Cowpertwait, P.S., O'Connell, P.E., 1997. A regionalised Neyman-Scott model of rainfall with convective and stratiform cells. Hydrol. Earth Syst. Sci. Discuss. 1 (1), 71–80.
Czemiel Berndtsson, J., 2010. Green roof performance towards management of runoff water quantity and quality: a review. Ecol. Eng. 36 (4), 351–360. http://dx.doi.org/10.1016/j.ecoleng.2009.12.014.
DeNardo, J.C., Jarrett, A.R., Manbeck, H.B., Beattie, D.J., Berghage, R.D., 2005. Stormwater mitigation and surface temperature reduction by green roofs. Trans. Am. Soc. Agric. Eng. 48 (4), 1491–1496.
Dietz, M.E., 2007. Low impact development practices: A review of current research and recommendations for future directions. Water Air Soil Pollut. 186 (1–4), 351–363. http://dx.doi.org/10.1007/s11270-007-9484-z.
Dvorak, B., Volder, A., 2010. Green roof vegetation for North American ecoregions: a literature review. Landscape Urban Plan. 96 (4), 197–213. http://dx.doi.org/10.1016/j.landurbplan.2010.04.009.
Entekhabi, D., Rodriguez-Iturbe, I., Eagleson, P.S., 1989. Probabilistic representation of the temporal rainfall process by a modified Neyman-Scott Rectangular Pulses Model: Parameter estimation and validation. Water Resour. Res. 25 (2), 295–302.
Feng, C., Meng, Q., Zhang, Y., 2010. Theoretical and experimental analysis of the energy balance of extensive green roofs. Energy Build. 42 (6), 959–965. http://dx.doi.org/10.1016/j.enbuild.2009.12.014.
Fioretti, R., Palla, A., Lanza, L.G., Principi, P., 2010. Green roof energy and water related performance in the Mediterranean climate. Build. Environ. 45 (8), 1890–1904. http://dx.doi.org/10.1016/j.buildenv.2010.03.001.
Getter, K.L., Rowe, D.B., 2006. The role of extensive green roofs in sustainable development. HortScience 41 (5), 1276–1285.
Getter, K.L., Rowe, D.B., Andresen, J.A., 2007. Quantifying the effect of slope on extensive green roof stormwater retention. Ecol. Eng. 31 (4), 225–231. http://dx.doi.org/10.1016/j.ecoleng.2007.06.004.
Hilten, R.N., Lawrence, T.M., Tollner, E.W., 2008. Modeling stormwater runoff from green roofs with HYDRUS-1D. J. Hydrol. 358 (3–4), 288–293. http://dx.doi.org/10.1016/j.jhydrol.2008.06.010.
Islam, S., Entekhabi, D., Bras, R., Rodriguez-Iturbe, I., 1990. Parameter estimation and sensitivity analysis for the modified Bartlett-Lewis rectangular pulses model of rainfall. J. Geophys. Res.: Atmos. 95 (D3), 2093–2100.
Laio, F., Porporato, A., Ridolfi, L., Rodriguez-Iturbe, I., 2001. Plants in water-controlled ecosystems: active role in hydrologic processes and response to water stress: II. Probabilistic soil moisture dynamics. Adv. Water Resour. 24 (7), 707–723.
Locatelli, L. et al., 2014. Modelling of green roof hydrological performance for urban drainage applications. J. Hydrol. 519 (PD), 3237–3248. http://dx.doi.org/10.1016/j.jhydrol.2014.10.030.
Milly, P.C.D., 1994. Climate, soil water storage, and the average annual water balance. Water Resour. Res. 30 (7), 2143–2156. http://dx.doi.org/10.1029/94wr00586.
Monterusso, M.A., Rowe, D.B., Rugh, C.L., Russell, D.K., 2004. Runoff water quantity and quality from green roof systems. Acta Hortic., 369–376
Palla, A., Gnecco, I., Lanza, L.G., 2009. Unsaturated 2D modelling of subsurface water flow in the coarse-grained porous matrix of a green roof. J. Hydrol. 379 (1–2), 193–204. http://dx.doi.org/10.1016/j.jhydrol.2009.10.008.
Palla, A., Gnecco, I., Lanza, L.G., 2012. Compared performance of a conceptual and a mechanistic hydrologic models of a green roof. Hydrol. Process. 26 (1), 73–84. http://dx.doi.org/10.1002/hyp.8112.
Puente, C., Bierkens, M., Diaz-Granados, M., Dik, P., López, M., 1993. Practical use of analytically derived runoff models based on rainfall point processes. Water Resour. Res. 29 (10), 3551–3560.
Rodriguez-Iturbe, I., Cox, D., Isham, V., 1987a. Some models for rainfall based on stochastic point processes, Proceedings of the Royal Society of London A: Mathematical, Physical and Engineering Sciences. The Royal Society, pp. 269-288.
Rodríguez-Iturbe, I., Power, B.F., Valdes, J.B., 1987b. Rectangular pulses point process models for rainfall: analysis of empirical data. J. Geophys. Res.: Atmos. 92 (D8), 9645–9656.
Šimůnek, J., van Genuchten, M.T., Šejna, M., 2008. Development and applications of the HYDRUS and STANMOD software packages and related codes. Vadose Zone J. 7 (2), 587–600.
Stovin, V., 2010. The potential of green roofs to manage urban stormwater. Water Environ. J. 24 (3), 192–199. http://dx.doi.org/10.1111/j.1747-6593.2009.00174.x.
Stovin, V., Poë, S., Berretta, C., 2013. A modelling study of long term green roof retention performance. J. Environ. Manage. 131, 206–215. http://dx.doi.org/10.1016/j.jenvman.2013.09.026.
Stovin, V., Vesuviano, G., Kasmin, H., 2012. The hydrological performance of a green roof test bed under UK climatic conditions. J. Hydrol. 414–415, 148–161. http://dx.doi.org/10.1016/j.jhydrol.2011.10.022.
Thornthwaite, C.W., 1948. An approach toward a rational classification of climate. Geograph. Rev. 38 (1), 55–94.
Verhoest, N., Troch, P.A., De Troch, F.P., 1997. On the applicability of Bartlett-Lewis rectangular pulses models in the modeling of design storms at a point. J. Hydrol. 202 (1), 108–120.
Viola, F. et al., 2016. Co-evolution of hydrological components under climate change scenarios in the Mediterranean area. Sci. Total Environ. 544, 515–524. http://dx.doi.org/10.1016/j.scitotenv.2015.12.004.
Viola, F., Pumo, D., Noto, L.V., 2014. EHSM: A conceptual ecohydrological model for daily streamflow simulation. Hydrol. Process. 28 (9), 3361–3372.
Voyde, E., Fassman, E., Simcock, R., 2010. Hydrology of an extensive living roof under sub-tropical climate conditions in Auckland, New Zealand. J. Hydrol. 394 (3–4), 384–395. http://dx.doi.org/10.1016/j.jhydrol.2010.09.013.
Wilby, R.L., 1999. The weather generation game: A review of stochastic weather models. Prog. Phys. Geogr. 23 (3), 329–357.